Two-Photon Laser Writing of Soft Responsive Polymers via Temperature-Controlled Polymerization

LASER & PHOTONICS REVIEWS

www.lpr-journal.org

Two-Photon Laser Writing of Soft Responsive Polymers via Temperature-Controlled Polymerization

Isabella De Bellis, Sara Nocentini, M. Giulia Delli Santi, Daniele Martella, Camilla Parmeggiani, Simone Zanotto, and Diederik S. Wiersma*

Enhancing the resolution of 3D patterning techniques in functional soft polymers enlarges the application areas of responsive shape-changing materials, for tunable nanophotonics and nanorobotics. Thanks to the recent advances of polymer science, the palette of available materials for nanomanufacturing is becoming wider and wider—although the comprehension of their polymerization process by two-photon polymerization is still incomplete. In this work, both shrinking of the minimal polymerizable unit and a significant improvement of the mechanical stability of microstructured soft polymers, in particular of liquid crystalline networks, are demonstrated. To this aim, temperature control enhances the resolution and reduces the swelling of the polymerized structures, thus avoiding deviations of the final structure from the intended design. This fine control on the nanoscale features enables the use of soft responsive materials not only for bulky microelements, but also for high-resolution structures with more complex design.

1. Introduction

Functionalized soft polymers represent an interesting platform for microdevices in biological,[1] biomedical,[2] fluidic,[3] photonic,[4] and robotic[5] applications. Their growth is motivated by their biocompatibility,[6,7] by their soft and adaptive nature, as well as by the possibility to chemically tailor their mechanical and optical properties.[8,9] The interest for miniaturization prompted us to shrink down various devices to the microscale—hence requiring high-resolution lithographic techniques as soft lithography and photolithography.[10] While these techniques offer good resolution in 2D structures, truly 3D designs in polymeric matrices can be obtained in a single-step process only by two-photon polymerization-based lithography, also called two-photon direct laser writing (DLW).[11] Increasing the dimensionality of soft structures requires a superior control over the writing process, since the concept of planar resolution is translated to three dimensions. At the same time, soft structures should retain the designed geometry during and after the writing process, issue that can be overcome by balancing the rigidity and mechanical stability of the polymerized resins.

In 3D photonic crystals,[12] chiral photonic structures,[13] as well as in optomechanics applications,[14] the typical structural critical size for visible and near-infrared applications ranges down to hundreds of nanometers. Furthermore, long-range regularity is required in photonic crystals and metasurfaces. This means that the polymerized structure must have a sufficient rigidity to avoid deformation effects that can occur while the full structure is written. Such a rigidity requirement conflicts with the softness that is intrinsic in responsive soft polymers; hence, the writing process must include a control mechanism, which is able to target the right balance over these opposite characteristics. Among responsive soft polymers, liquid crystalline networks (LCNs)[15,16] gained great attention for their striking characteristic of large controllable deformations introduced by diverse actuation sources. Using an external stimulus as temperature,[10] pH,[17] or light,[18] switching among liquid crystalline phases can be reversibly attained, thus obtaining a shape deformation that depends on the programmed molecular alignment.[19,20] Such responsiveness to external stimuli has been exploited in soft actuators and artificial-muscle-based applications,[21] and extended to tunable photonic devices.[22] While 4D printing of LCEs (liquid

Dr. I. De Bellis, Dr. S. Nocentini, Dr. D. Martella, Dr. C. Parmeggiani, Prof. D. S. Wiersma
European Laboratory for Non-Linear Spectroscopy (LENS)
University of Florence
Via Nello Carrara 1, Sesto Fiorentino 50019, Italy

Dr. S. Nocentini, Dr. D. Martella, Dr. C. Parmeggiani, Prof. D. S. Wiersma
Istituto Nazionale di Ricerca Metrologica INRiM
Strada delle Cacce 91, Turin 10135, Italy
E-mail: s.nocentini@inrim.it

Dr. M. G. Delli Santi
CNR-INO
Via Nello Carrara 1, Sesto Fiorentino 50019, Italy

Dr. C. Parmeggiani
Department of Chemistry "Ugo Schiff,"
University of Florence
Via della Lastruccia 3–13, Sesto Fiorentino 50019, Italy

Dr. S. Zanotto
Istituto Nanoscienze - CNR and NEST - Scuola Normale Superiore
Piazza S. Silvestro 12, Pisa 56127, Italy

Prof. D. S. Wiersma
Department of Physics and Astronomy
University of Florence
Via Sansone 1, Sesto Fiorentino 50019, Italy

The ORCID identification number(s) for the author(s) of this article can be found under https://doi.org/10.1002/lpor.202100090

DOI: 10.1002/lpor.202100090

crystalline elastomers) have been widely explored in millimetric and micrometric actuators by using different techniques and chemical formulations,[23–28] only a few examples of liquid crystalline networks patterned with DLW have been recently reported for robotic[29–31] and photonic applications,[32–35] but their further development is still limited by the resolution and the mechanical property control. Another important class of responsive polymers is hydrogels (HGs). They are crosslinked hydrophilic polymers that show a significant isotropic shape change during swelling in water-based media. Recent works demonstrated both as DLW HG microstructures that can change their shape in response to temperature or light[36] and how water erasable structures can be prepared by a proper polymer modification.[37] The fact that hydrogels swell greatly in fluids can be used in microfluidics,[38,39] robotic microswimmers,[40] and biological applications.[38,41] Microstructured HGs suffer from the same restrictions of LCNs, and their resolution is of a few hundreds of nanometers.[42,43] Thus, lithographic performances on soft polymers have to be improved toward the results obtained for glassy commercial resists—still preserving their peculiar elasticity—in order to make them really competitive and appealing for nanostructured devices. By tuning the lithographic setting and varying the chemical composition of the monomer mixture, a lateral resolution of 160 nm can be achieved.[44] Furthermore, to reduce the smallest polymerizable unit (namely the voxel, volume pixel), different strategies have been proposed either exploiting the addition of polymerization inhibitors[45] or translating the stimulated-emission depletion (STED) fluorescence microscopy principle into the lithographic analog.[46] Despite the obtained resolution that gets closer to 70 nm, such methods require tailored molecular formulations and/or complex optical setup that cannot be used for every type of photopolymerizable mixture.

Surprisingly, one of the most easily controllable patterning parameters, which is temperature, has been mostly overlooked to date. Several phenomena (e.g., swelling, polymerization shrinkage, and monomer diffusion) have temperature dependence; hence, they are definitely expected to contribute to determine the voxel dimensions. In particular, diffusion of the liquid monomers affects both structural resolution and rigidity. In addition to intrinsic material properties, monomer diffusion depends on external parameters as temperature.[47] Interestingly, the light-induced polymerization with high-power femtosecond lasers does not induce a significant local heating of the exposed volume; such heating has been estimated to be smaller than 5 °C for laser powers well above the polymerization threshold. This confirmed the photochemical nature of the polymerization process itself, rather than a photothermal one.[48] An external temperature control over the process should then be achieved by a customized heating/cooling system. Kawata and co-workers carried out temperature-dependent polymerization characterization on commercial resins, demonstrating that the reduction of temperature slightly lowers the voxel size, while the increase of temperature leads to improved resolution (from 1.4 μm at 20 °C to 1 μm at 80 °C for 512 ms exposure time).[49] Such a behavior has been attributed to a reduction of the monomer diffusion at negative temperatures whereas, at higher temperatures, the accelerated termination of the polymerization reaction improved the lateral resolution.[49] This analysis is still limited to commercial and glassy materials, and it is of great interest to generalize it for certain responsive materials of technological relevance to enlarge their application field.

In this work, we present a DLW implementation as an enabling method for nanopatterning soft deformable polymers with resolution and design reproducibility comparable to commercial glassy resins. A temperature-dependent analysis of photopolymerization on shape-changing birefringent polymers (LCNs; Figure S1, Supporting Information), and hydrogels (poly(ethylene glycol) (PEG); Figure S2, Supporting Information) with respect to a commercial glassy polymer (IP-Dip, Nanoscribe GmbH; Figure S3, Supporting Information) highlighted the importance of this parameter to increase resolution and reduce structure deformation due to swelling.

2. Results and Discussion

In order to improve the lithographic performances of custom mixtures, chemical modifications that include the introduction of a polymerization quencher and different types of photoinitiators have been first tested before investigating the temperature role in two-photon polymerization. The polymerization quencher (2-(dimethylamino)ethyl methacrylate)[45] has been added into the liquid crystalline mixture (see Figures S4 and S5 in the Supporting Information). Within this strategy, the resolution was not notably outperformed while the structure rigidity considerably decreased, getting us away from the research goal. This behavior can be explained as follows: the quencher inhibits the polymerization as well as the crosslinking process making the structures softer and therefore not more suitable for self-standing devices. Resolution control has also been explored by varying the type of photoinitiator (see Figure S6 in the Supporting Information). Such an analysis underlined as the best choice for the photoinitiator is Irgacure 369 (Sigma–Aldrich) that allows us to operate in a wide window of parameters (writing speed and laser power; see Figure S7 in the Supporting Information) leading to high-resolution structures in elastic materials, which however possess enough rigidity (Figure S9, Supporting Information) to be patterned in suspended designs.

To further control resolution, we exploited the dependence on temperature of the chemical–physical properties of stimuli–responsive shape-changing materials (LCNs and HGs). In our study, the investigated temperatures were between 5 °C and room temperature. This choice allowed us to maintain a stable liquid crystal (LC) nematic phase on the LCN samples—indeed, the LCN mixture with a 30% mol/mol of crosslinker content shows a wide nematic phase window from 50 down to 0 °C.[50] Writing structures in such an interval freezes the desired alignment into the final polymerized device. We investigated planar homogeneously (liquid crystalline molecules parallel to the glass substrate) or homeotropically (liquid crystalline molecules orthogonal to the glass substrate) aligned structures as the most widely exploited molecular orderings that originate contraction movement (parallelly and orthogonally to the substrate, respectively). The sample preparation for the three different resist cells (i.e., LCN-, HG-, and IP-Dip-filled cells) and the scheme of the homemade Peltier stage implementation are reported in **Figure 1**a and in Figures S10 and S11 (Supporting Information).

The main experimental features connected, on one side, to the lithographic performance, and on the other side, to the molecular

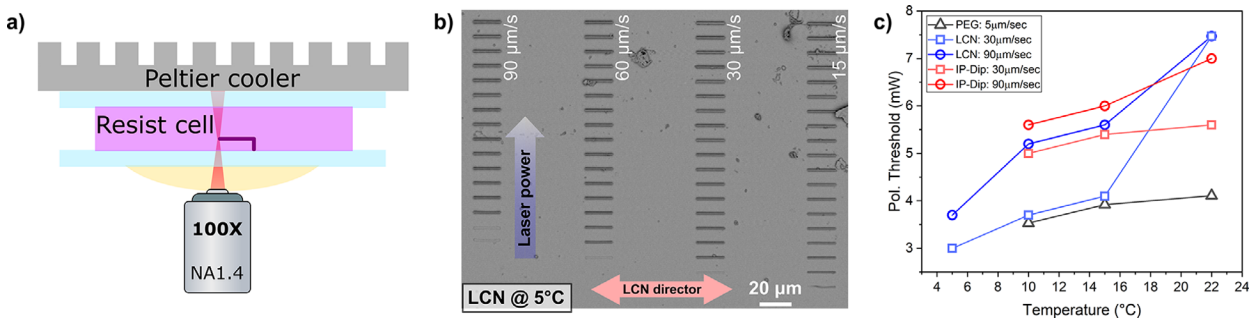

Figure 1. Polymerization Threshold. a) Scheme of the temperature-controlled direct laser writing. b) SEM image of a polymerization threshold characterization for the LCN homogeneously planar aligned mixture. The 20 µm segments have been written at the glass–resist interface varying the writing speed (from left to the right) and increasing the laser power (from the bottom to the top of the image). The shown characterization was done at 5 °C. c) Polymerization thresholds for the different mixtures (HG, LCN, and IP-Dip) as a function of temperature. Two different writing speeds are reported for the LCN and IP-Dip resists.

dynamics and the physical–chemical process are the polymerization threshold, the voxel dimensions (planar and vertical resolutions), and the structure rigidity. Such quantities are observed in DLW experiments performed by varying the temperature, the lithographic writing speed, and the laser power value.

The polymerization threshold, given a certain writing velocity, is the lowest power value able to create a well-defined polymeric line at the glass–resist interface. 20 µm long lines have been fabricated at the glass–resist interface varying the polymerization temperature from 22 to 5 °C, and the laser power value for each segment at a fixed writing speed (from 90 to 15 µm s^{-1}). A scanning electron microscope (SEM) image of such printing calibration is reported in Figure 1b for the elastomeric mixture at 5 °C and in Figure S12 (Supporting Information) at 22 °C. From this experiment, we observed that for the IP-Dip resist and the hydrogel mixture, only a small variation of the polymerization threshold occurs; the polymerization threshold remains almost constant within this temperature range (Figure 1c). A relevant dependence has been found instead for liquid crystalline networks, whose polymerization threshold passes from around 7.5 mW at room temperature down to 3 mW at 5 °C (Figure 1c). At a glance, polymerization threshold may be mainly attributed to the activation of the photoinitiator, but it is inherently defined by the termination kinetics and molecular reactivity.[47,51] The kinetic behavior is dominated by photoinitiator depletion and radical quenching.[52,53] The model that describes the photopolymerization process relies on a system of partial differential equations for the photoinitiator, the monomer, the radical, and the general inhibiting molecules' concentration.[46] Once the initial concentrations of each species, the incident laser flux, and the different quantum yields are fixed, the parameters that affect the polymerization are the diffusions of each molecule type and the termination constants (due to radical–radical termination, radical trapping in the polymeric network, and combination of radical with inhibiting molecules, as oxygen).[51] For liquid crystalline network formation, the temperature decrease favors polymerization at lower laser power. In principle, this could be explained as a reduction of the diffusion coefficients, enhanced molecule reactivity, or a more efficient termination kinetics. As the last two contributions decrease with temperature according to the Arrhenius law,[51] the dominant effect should be attributed to a reduced molecular diffusion that promotes the formation of a solid voxel. This effect is evident only for the LCN mixture probably, because, in the considered temperature range, the diffusion coefficients vary more considerably, getting closer to the glass temperature. Thus, lowering the temperature, monomers and radicals have a reduced diffusion coefficient that promotes the termination of the polymeric chains; hence, reducing the laser power needed to induce the photopolymerization.

To further explore this peculiar trend, we investigated the voxel dimension's variation as a function of temperature. Improving the 3D DLW resolution implies to minimize both the lateral resolution and the vertical one as well. In fact, a spheroidal voxel would be the best polymerization unit to fabricate 3D structures, especially in 3D photonic structures as woodpile crystals or chiral photonic crystals for which isotropic voxel dimensions are definitely welcomed. Due to the nonlinear photoabsorption in the focal volume of the laser beam, the polymerization unit has an ellipsoidal shape, whose aspect ratio (ratio of the major and minor axes of the voxel) should be brought, in principle, as close as possible to unity. For commercial resists, an aspect ratio of 2.7 is a reference value.[54] The resolution has been evaluated from suspended lines fabricated on square grids of 20 µm in size, varying the writing velocity and the laser power (**Figure 2**a).

Analyzing the SEM images, both the minor and the major axis have been measured and reported as a function of the writing power and of the temperature in Figure 2b,c. For LCN compounds, by controlling both the polymerization power and temperature, the lateral resolution of the suspended lines can be pushed below 120 nm by decreasing the temperature of the monomeric mixture down to 10 °C (Figure 2b). The lateral resolution does not show a significant dependence on temperature for the IP-Dip resist (Figure 2c), reaching at the polymerization threshold, a voxel's minor axis of 130 nm (writing speed 90 µm s^{-1}). A similar behavior has been found for PEG mixture. Also the major axis follows this trend, thus enabling the fabrication of more spheroidal voxels (Figure 2d; Figure S13, Supporting Information). At room temperature, the best writing parameters create a voxel height of around 700 nm whereas at 10 °C, it decreases up to 390 nm (Figure S14, Supporting Information). Lowering the temperature leads to a reduction of the aspect ratio of LCN lines from 5 to 3 regardless of the employed power, thus making it comparable with the values obtained for commercial resists (Figure 2e). The significant aspect ratio reduction of LCN lines could

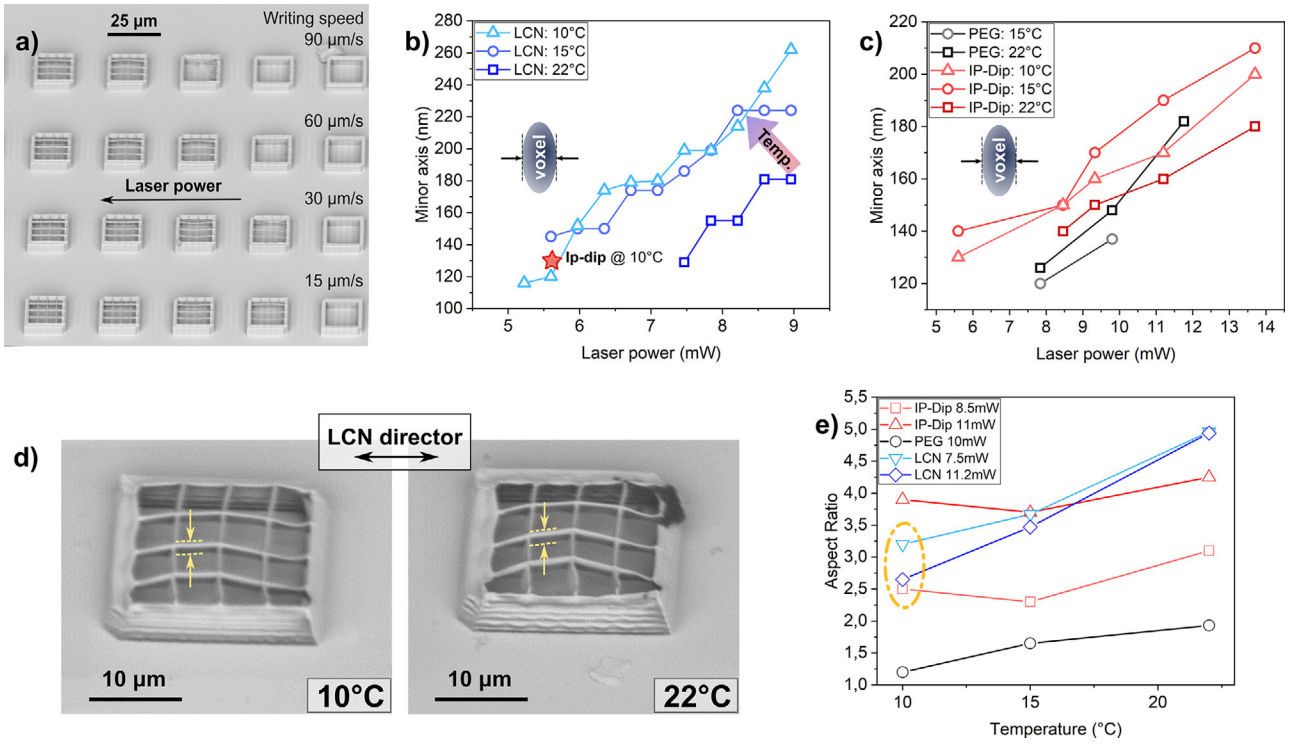

Figure 2. a) SEM image of a series of suspended grids to evaluate the line minor and major axes of the IP-Dip resist at room temperature. The writing parameters are varied: laser power increased from right to left, and the laser scanning speed from the bottom to the top. b) Voxel minor axis as a function of power for the LCN homogeneously planar aligned mixture at different writing temperatures. The best resolution obtained with the commercial IP-Dip resin is indicated by the red star. c) Voxel minor axis as a function of power for the PEG hydrogel and IP-Dip mixtures at different writing temperatures. d) SEM image that shows the major axis reduction at the lowest temperature (10 °C) for the LCN mixture in a homogeneous cell. e) Evaluated aspect ratio (ratio between the major and the minor voxel axis) as a function of temperature for the three resists at different writing powers. In the yellowish dash-dot region, it is highlighted that the best resolution performances of LCNs are comparable with the commercial resist (IP-Dip).

be attributed to physical–chemical properties of liquid crystalline materials as well as to the anisotropic nature of the mixture that is further analyzed in the text. On the other hand, for isotropic resins such as IP-Dip and HG, the temperature-controlled polymerization is a not effective tool in controlling the aspect ratio. The best resolution and aspect ratio are achieved for the hydrogel mixture, whose aspect ratio at 10 °C describes an almost spherical voxel. These achievements broaden the range of applications of LCNs and HGs to any kind of 3D structures with both the resolution and the geometrical feature improved toward the performances of well-known commercial polymers.

With a further look at Figure 2d, another effect can be noticed; decreasing the temperature, the suspended lines become more parallel, thus better reproducing the intended structure design. We hence decided to undergo a systematic analysis of this effect that can be better appreciated in LCNs (**Figure 3**a). The segment's bending of soft materials in the photopolymerization process is due to the swelling of the unpolymerized monomers inside the crosslinked network. This liquid penetration into the solid elements leads to a line warping that is definitely undesirable within a lithographic process. The idea is here that, by reducing the temperature of the liquid mixture, the diffusion of monomers inside the polymerized volume is reduced accordingly. This effect has been evaluated through a quantitative estimation of the line warping. Line warping is defined as the deviation from linearity, as shown in Figure 3a, and quantitatively estimated in Figure 3b. It has been quantified by measuring the lateral displacement of the first written line of the grid. This choice is motivated by the fact that the first written segment of the grid has more time to deform compared to the other lines (about 10 s). Only the warping of horizontal lines has been considered, as vertical lines have been written later; hence, they were forced not to warp by the existing constraint (the intersection with the horizontal lines).

The deformation is larger along the direction perpendicular to the director, as demonstrated in Figure 3c, which shows suspended lines, parallel and perpendicular to the director direction, written at room temperature with a writing speed of 90 μm s^{-1}, and varying the laser power. This phenomenon can be explained by considering that the Young's modulus is higher along the director direction than the perpendicular one ($E_{\perp} < E_{//}$).[55] In the case of the employed LCN mixture, Young's modulus of the polymerized structure also increases as an order of magnitude from 22 to 5 °C justifying the rigidity increase with the temperature decrease.[50] At the same time, the diffusion of monomers decreases with temperature (with $D_{\perp} < D_{//}$). It can, hence, be expected that the dynamics of line warping is dependent on the temperature; indeed, this was confirmed by the data shown in Figure 3d. Here it is reported the time evolution of the warping of a single suspended line immediately after it has been written, when it is still inside the cell, immersed in the undeveloped

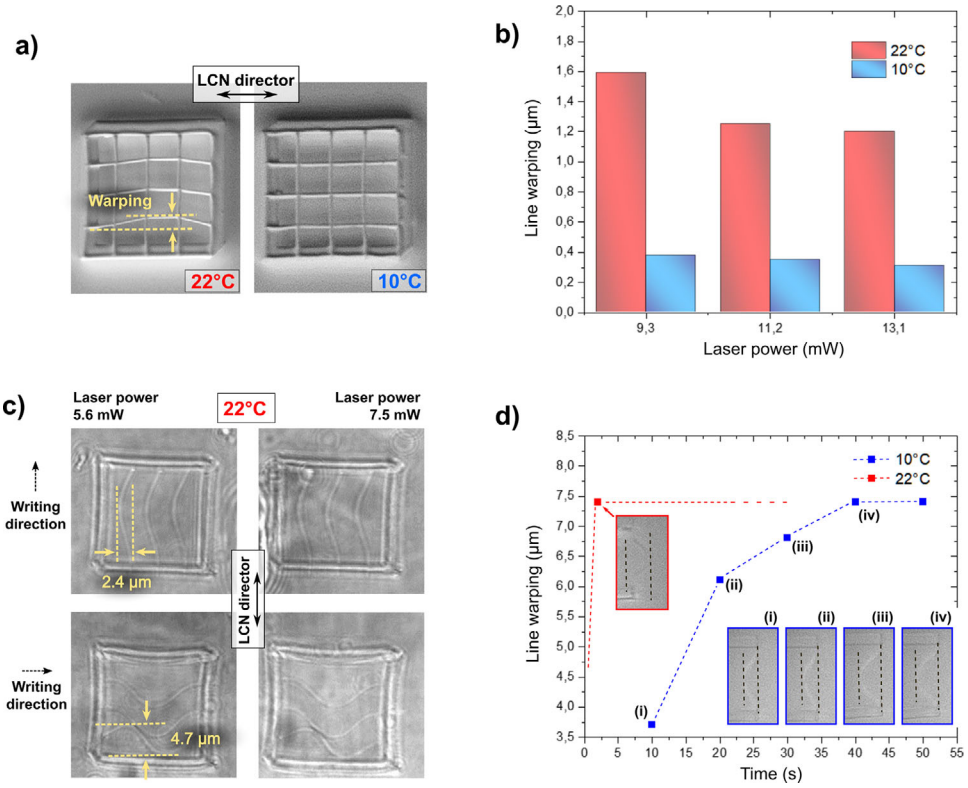

Figure 3. Swelling in LCN structures. a) SEM images of the grids fabricated in LCN mixture with a homogeneous planar alignment at 22 and 10 °C showing the line warping effect. b) Line warping as a function of laser power for the first line written parallel to the director in homogeneous planar aligned grids at 22 and 10 °C, respectively. c) Suspended lines parallel to the director direction fabricated in a homogeneous planar cell showing a lower line warping than perpendicular ones. d) Time evolution of the line warping of suspended lines written in a homogeneous planar cell at 22 and 10 °C. Images in panel (a) are obtained with scanning electron microscopy of the developed sample, while images in panels (c) and (d) are collected through the objective of the direct laser writing apparatus from the LCN cell before development.

mixture. At 22 °C, the line reaches the maximum warping in less than 2 s; instead, at 10 °C, the maximum line warping is reached in about 40 s. It should be noticed that the maximum warping is almost the same for both temperatures (i.e., about 7.5 μm for a line with a length of 20 μm).

In literature, the reduction of line warping is attributed to the increase of laser power that favors a more efficient crosslinking degree. However, the laser power to increase the degree of polymerization and crosslinking results detrimental in terms of resolution.[56] Here we demonstrated how to reduce swelling simply by lowering the temperature, thanks to a reduced monomer diffusion and to the Young's modulus temperature dependence. In such a way, a more efficient polymerization process is achieved improving both the resolution and the structures' rigidity. Moreover, the benefits of the improved resolution and mechanical properties by DLW at 10 °C allowed the fabrication of free-standing elements with only one edge attached to a bulk polymeric wall (Figure S15, Supporting Information). This study is the proof of concept that low-temperature polymerization allows the fabrication of more rigid suspended elements in an LCN matrix, opening the way to 3D shape changing photonic structures.

A careful analysis of the voxel dimensions unearthed another interesting behavior for DLW-patterned LCNs. In an LC-aligned cell, the voxel dimensions depend on the writing direction with respect to the LC director, while the other isotropic resists do not express such dependence. In the following, we provide a detailed analysis of the phenomenon, which can be attributed to the isotropy/anisotropy of the underlying molecular matrices. A scheme of the LCN grids is reported in **Figure 4**a, with the effect being exaggerated to clarify the observed results. We investigated such a phenomenon using both a homogeneous and a homeotropic alignment.

First of all, we verified that the laser writing direction does not perturb the alignment of the LC cell impressed by the sacrificial layers.[57] In Figure S16 (Supporting Information), 3D photonic structures have been polymerized in a homogeneous planar cell (Figure S16a, Supporting Information) and in an homeotropic cell (Figure S16b, Supporting Information) showing that the laser writing direction does not affect the final alignment of the structures. Indeed, both polarized optical microscope images and the contraction of the structures (Figure S16c, Supporting Information) are ruled by the LC alignment preimpressed by the alignment layer of the cell and not the laser writing direction.

Let us first analyze the results observed in the case of homogeneous alignment. Figure 4b shows that, if the writing direction is parallel to the molecular alignment, the polymerized lines are characterized by a considerably larger major axis and a shorter minor axis. The dimensions of the minor axis of orthogonally realized lines, in homogeneous and homeotropic LC cells, are

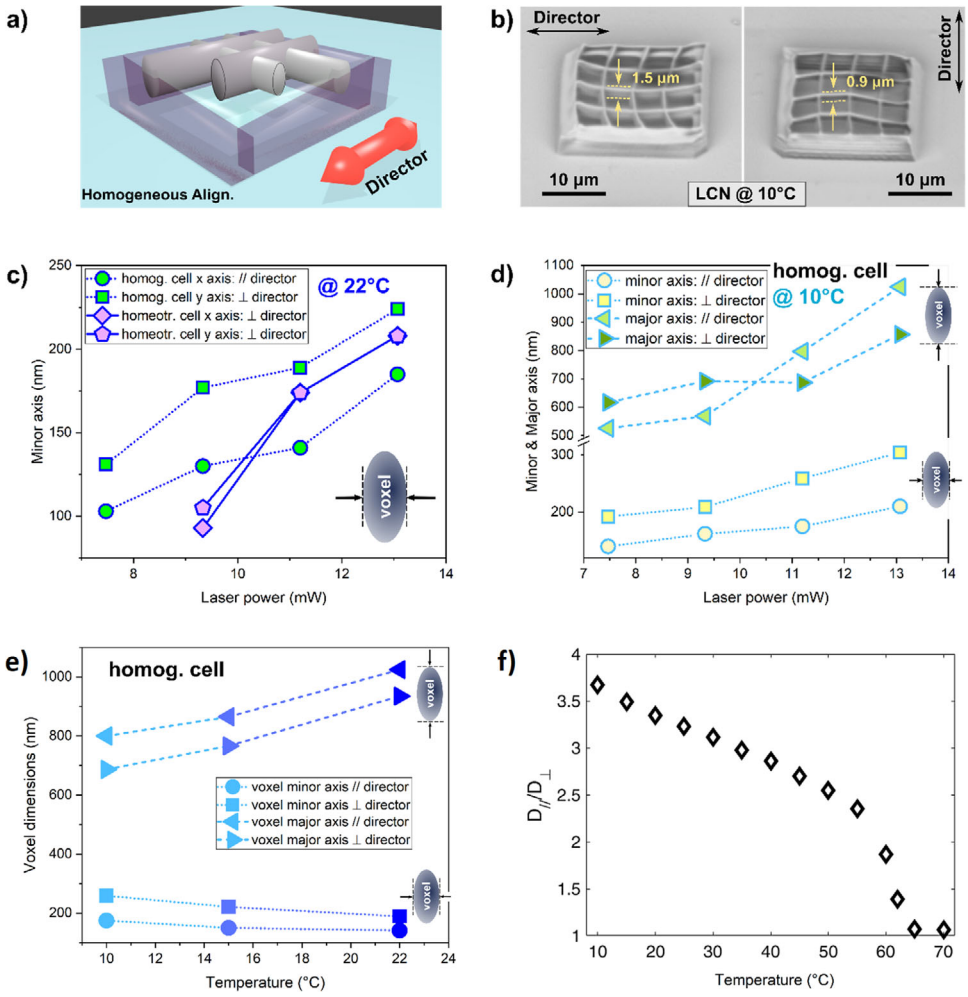

Figure 4. Anisotropic resolution in LCN mixture. a) Scheme of the anisotropic line resolution in a homogeneous planar aligned LC cell. b) SEM pictures of the grid realized in an LCN mixture at 10 °C, whose lines have been written parallel and orthogonally to the director direction in a homogeneous planar cell. c) Minor axis size as a function of writing power for a homogeneous planar and homeotropic aligned cell. The laser writing was performed at 22 °C. d) The sizes of minor and major axes as a function of writing power for a homogeneous planar aligned cell. The laser writing was performed at 10 °C. e) The minor and the major axis variation with temperature. The size is reported for lines polymerized written parallelly and normally to the director direction in a homogeneous planar cell. The lithographic parameters are fixed: laser power 11.2 mW, writing speed 90 µm s^{-1}. f) Calculated diffusion coefficient ratio between the parallel and the orthogonal components with respect to the LC director as a function of temperature.

measured and reported in Figure 4c for grids polymerized at room temperature (the major axis dimensions are reported in Figure S17 in the Supporting Information). In homeotropic cells (purple dashed lines), with the director orthogonal to the glass substrate, both the minor and the major axis of the two differently oriented lines remain equal within the estimated error (30 nm), as expected. Such observations underline that the voxel dimensions are affected by the liquid crystalline molecule's orientation. When the director lies in the x–y plane, the in-plane molecular anisotropy determines the polymerized voxel dimensions, while in the homeotropic case no differences are present. The laser writing direction does not influence the dimension of the voxel itself. To verify the influence of the molecular anisotropy also at a reduced writing temperature (10 °C), we reported the values of the minor and the major axis of suspended lines in a homogeneous cell as shown in Figure 4d. Also in this case, the voxel anisotropy is more pronounced. The first evidence of this anisotropy was already reported in literature, showing that if the DLW writing direction is parallel to the LC alignment, the resulting lines are thicker and do not present any visible curl along the alignment direction.[58] Also the polymerization shrinkage, which is the volume contraction due to the polymerization, depends on the molecular orientations and the temperature, and it is responsible for the final size of the polymerized structures.[59,60] However, the main influence is probably due to the anisotropy of monomer diffusion. In fact, in the homogeneous alignment, the different segment thicknesses, obtained parallelly and perpendicularly to the director, can be explained by the anisotropy of the self-diffusion coefficients in liquid crystalline mixtures.[61,62] In nematic liquid crystals, the diffusion coefficient $D_{//}$ parallel to the liquid crystal director is larger than the orthogonal component $D_{\perp}$.[62] A higher rate of molecule diffusion along the LC orientation, together with the high anisotropy of the molecule dimensions, affects the voxel

dimension that is thinner and taller when the writing direction is parallel to the LC director.

Such an intriguing behavior has been then investigated for different writing temperatures. The voxel dimensions have been evaluated at different temperatures in a homogeneous cell along the director and orthogonally to it (Figure 4e). When the sample temperature is brought to 10 °C, considering the writing direction being parallel to the director, the voxel minor axis slightly increases in size while its major axis decreases by more than 100 nm. The same behavior is retrieved also for the writing direction perpendicular to the director (Figure 4e). For both writing directions, the major axis is significantly reduced creating a more spheroidal voxel, one of the key achievements in nanopatterning. A possible explanation, besides the temperature dependence of the polymerization of LCN, was sought in the material anisotropy.

To this end, we compared our experimental results with the models that predict the temperature dependence of the diffusion coefficients. Molecular diffusion in isotropic and nematic phases follows a well-known behavior; the temperature dependence of the diffusion coefficient, in the isotropic phase, retains an Arrhenius-type trend,[63] while in the mesophase, $D_{//} > D_{\perp}$, as successfully described by the Hess–Frenkel–Allen (HFA) model[61] and by the Chu and Moroi (CM) model.[64] To check how the ratio of the two diffusion constants changes with temperature, we exploited the HFA model to retrieve the temperature dependence as it was already demonstrated good accordance with experimental results.[63] We measured the order parameter, S, as a function of temperature (see Figure S18 in the Supporting Information) to monitor the temperature variation of the LC anisotropy. From these experimentally retrieved values, we calculated the temperature dependence of the ratio of the two self-diffusion coefficients ($D_{//}/D_{\perp}$) (see the Supporting Information) in our nematic liquid crystalline mixture using the HFA model (Figure 4f). The ratio of the two diffusion components increases with increasing molecular anisotropy while lowering the temperature. In light of such an increase, we can assume that, while temperature is decreased, the most significant variation is due to the $D_{\perp}$ reduction that shrinks down the major axis of the voxel, therefore reducing the resulting aspect ratio.

3. Conclusions

Controlling the temperature, at which a liquid crystal network (LCN) and a hydrogel are nanopatterned through two-photon polymerization (i.e., direct laser writing), enables us to define the shape and size of the 3D polymerizable unit (voxel). We explored, in detail, the effects of temperature on the polymerization threshold, on the voxel size and aspect ratio, on the line warping, and on the line thickness anisotropy. We have recognized in the temperature dependence of the anisotropic diffusion coefficient the key mechanism behind our observations concerning LCNs. Our results, in addition to the fundamental interest for the physical–chemical process of two-photon polymerization of LCNs and HGs, significantly improve the possibilities for the exploitation of these responsive polymers in nanopatterned structures. By implementing these concepts, the obtained resolution becomes comparable to that of commercial resists as well as the fidelity of the replica to the intended design, and the fabrication process governed by an additional degree of freedom can now be implemented for nanostructures in soft responsive materials.

4. Experimental Section

Direct Laser Writing System: The characterization was performed using the commercial platform for DLW (Nanoscribe GmbH) with a home-made Peltier stage (*RS* components) adapted to the sample holder with mechanical components. The temperature feedback controller was allowed to stabilize the writing temperature at a desired value (Figure S10, Supporting Information). The implementation of the temperature controller into the Nanoscribe system is reported with further details in the Supporting Information.

Materials: The characterization of the nanopatterned elements was performed using three different material formulations: IP-Dip, a commercial resist developed by Nanoscribe GmbH, polyethylene glycol diacrylate (average $M_n = 250$), and a liquid crystalline network mixture. The molecular composition and sample preparation is reported in detail in the Supporting Information.

Characterization: The nanostructures fabricated by DLW were imaged by a tabletop scanning electron microscope (Phenom G1) and a polarized optical microscope (Zeiss, AXIO Observer.A1), and the images were analyzed by using the software ImageJ.

Supporting Information

Supporting Information is available from the Wiley Online Library or from the author.

Acknowledgements

I.D.B. and S.N. contributed equally to this work. The research leading to these results received funding from Ente Cassa di Risparmio di Firenze (2020/1583, 2018/1047), Fondo di Beneficenza Intesa San Paolo 2019 to the project "Multifunctional Optofluidic Devices for the Early Stage Diagnosis of Alzheimer's Disease through the Molecular Screening of Cerebrospinal Fluid—DOPTOSCREEN" (B/2019/0289), and Fondo premiale FOE to the project "Volume Photography: Measuring Three Dimensional Light Distributions without Opening the Box" (E17G17000300001).

Conflict of Interest

The authors declare no conflict of interest.

Data Availability Statement

Research data are not shared.

Keywords

direct laser lithography, hydrogel, liquid crystalline networks, soft responsive polymers, temperature dependence

Received: February 17, 2021
Revised: May 13, 2021
Published online:

[1] R. K. Iha, K. L. Wooley, A. M. Nystrom, D. J. Burke, M. J. Kade, C. J. Hawker, *Chem. Rev.* **2009**, *109*, 5620.

[2] E. Smela, *Adv. Mater.* **2003**, *15*, 481.
[3] C. F. Carlborg, T. Haraldsson, K. Öberg, M. Malkoch, W. van der Wijngaart, *Lab Chip* **2011**, *11*, 3136.
[4] A. C. Edrington, A. M. Urbas, P. DeRege, C. X. Chen, T. M. Swager, N. Hadjichristidis, M. Xenidou, L. J. Fetters, J. D. Joannopoulos, Y. Fink, E. L. Thomas, *Adv. Mater.* **2001**, *13*, 421.
[5] L. Hines, K. Petersen, G. Z. Lum, M. Sitti, *Adv. Mater.* **2017**, *29*, 1603483.
[6] J. F. Lutz, *J. Polym. Sci., Part A: Polym. Chem.* **2008**, *46*, 3459.
[7] D. Martella, P. Paoli, J. M. Pioner, L. Sacconi, R. Coppini, L. Santini, M. Lulli, E. Cerbai, D. S. Wiersma, C. Poggesi, C. Ferrantini, *Small* **2017**, *13*, 1702677.
[8] D. W. Smith Jr., S. Chen, S. M. Kumar, J. Ballato, C. Topping, H. V. Shah, S. H. Foulger, *Adv. Mater.* **2002**, *14*, 1585.
[9] M. A. C. Stuart, W. T. Huck, J. Genzer, M. Müller, C. Ober, M. Stamm, G. B. Sukhorukov, I. Szleifer, V. V. Tsukruk, M. Urban, F. Winnik, *Nat. Mater.* **2010**, *9*, 101.
[10] A. Buguin, M. H. Li, P. Silberzan, B. Ladoux, P. Keller, *J. Am. Chem. Soc.* **2006**, *128*, 1088.
[11] M. Deubel, G. Von Freymann, M. Wegener, S. Pereira, K. Busch, C. M. Soukoulis, *Nat. Mater.* **2004**, *3*, 444.
[12] A. Ledermann, L. Cademartiri, M. Hermatschweiler, C. Toninelli, G. A. Ozin, D. S. Wiersma, M. Wegener, G. von Freymann, *Nat. Mater.* **2006**, *5*, 942.
[13] M. Thiel, G. von Freymann, M. Wegener, *Opt. Lett.* **2007**, *32*, 2547.
[14] E. Descrovi, F. Pirani, V. P. Rajamanickam, S. Licheri, C. Liberale, *J. Mater. Chem. C* **2018**, *6*, 10428.
[15] J. Küpfer, H. Finkelmann, *Macromol. Rapid Commun.* **1991**, *12*, 717.
[16] M. H. Li, P. Keller, *Philos. Trans. R. Soc., A* **2006**, *364*, 2763.
[17] K. D. Harris, C. W. Bastiaansen, J. Lub, D. J. Broer, *Nano Lett.* **2005**, *5*, 1857.
[18] M. H. Li, P. Keller, B. Li, X. Wang, M. Brunet, *Adv. Mater.* **2003**, *15*, 569.
[19] T. Ikeda, J. I. Mamiya, Y. Yu, *Angew. Chem., Int. Ed.* **2007**, *46*, 506.
[20] T. J. White, D. J. Broer, *Nat. Mater.* **2015**, *14*, 1087.
[21] S. Nocentini, C. Parmeggiani, D. Martella, D. S. Wiersma, *Adv. Opt. Mater.* **2018**, *6*, 1800207.
[22] G. Wu, Y. Jiang, D. Xu, H. Tang, X. Liang, G. Li, *Langmuir* **2010**, *27*, 1505.
[23] X. Lu, C. P. Ambulo, S. Wang, L. K. Rivera-Tarazona, H. Kim, K. Searles, T. H. Ware, *Angew. Chem., Int. Ed. Engl.* **2021**, *60*, 5536.
[24] M. Barnes, S. M. Sajadi, S. Parekh, M. M. Rahman, P. M. Ajayan, R. Verduzco, *ACS Appl. Mater. Interfaces* **2020**, *12*, 28692.
[25] N. A. Traugutt, D. Mistry, C. Luo, K. Yu, Q. Ge, C. M. Yakacki, *Adv. Mater.* **2020**, *32*, 2000797.
[26] M. López-Valdeolivas, D. Liu, D. J. Broer, C. Sánchez-Somolinos, *Macromol. Rapid Commun.* **2018**, *39*, 1700710.
[27] A. Kotikian, R. L. Truby, J. W. Boley, T. J. White, J. A. Lewis, *Adv. Mater.* **2018**, *30*, 1706164.
[28] M. del Pozo, L. Liu, M. Pilz da Cunha, D. J. Broer, A. P. Schenning, *Adv. Funct. Mater.* **2020**, *30*, 2005560.
[29] S. Palagi, A. G. Mark, S. Y. Reigh, K. Melde, T. Qiu, H. Zeng, C. Parmeggiani, D. Martella, A. Sanchez-Castillo, N. Kapernaum, F. Giesselmann, D. S. Wiersma, E. Lauga, P. Fischer, *Nat. Mater.* **2016**, *15*, 647.
[30] H. Zeng, P. Wasylczyk, C. Parmeggiani, D. Martella, M. Burresi, D. S. Wiersma, *Adv. Mater.* **2015**, *27*, 3883.
[31] D. Martella, S. Nocentini, D. Nuzhdin, C. Parmeggiani, D. S. Wiersma, *Adv. Mater.* **2017**, *29*, 1704047.
[32] A. M. Flatae, M. Burresi, H. Zeng, S. Nocentini, S. Wiegele, C. Parmeggiani, H. Kalt, D. Wiersma, *Light: Sci. Appl.* **2015**, *4*, e282.
[33] M. D. Pozo, C. Delaney, C. W. Bastiaansen, D. Diamond, A. P. Schenning, L. Florea, *ACS Nano* **2020**, *14*, 9832.
[34] S. Nocentini, D. Martella, C. Parmeggiani, S. Zanotto, D. S. Wiersma, *Adv. Opt. Mater.* **2018**, *6*, 1800167.
[35] S. Nocentini, F. Riboli, M. Burresi, D. Martella, C. Parmeggiani, D. S. Wiersma, *ACS Photonics* **2018**, *5*, 3222.
[36] M. Hippler, E. Blasco, J. Qu, M. Tanaka, C. Barner-Kowollik, M. Wegener, M. Bastmeyer, *Nat. Commun.* **2019**, *10*, 232.
[37] H. A. Houck, P. Müller, M. Wegener, C. Barner-Kowollik, F. Du Prez, E. Blasco, *Adv. Mater.* **2020**, *32*, 2003060.
[38] S. Cosson, M. P. Lutolf, *Sci. Rep.* **2014**, *4*, 4462.
[39] L. D'eramo, B. Chollet, M. Leman, E. Martwong, M. Li, H. Geisler, J. Dupire, M. Kerdraon, C. Vergne, F. Monti, Y. Tran, *Microsyst. Nanoeng.* **2018**, *4*, 17069.
[40] A. Nishiguchi, A. Mourran, H. Zhang, M. Möller, *Adv. Sci.* **2018**, *5*, 1700038.
[41] R. A. Barry III, R. F. Shepherd, J. N. Hanson, R. G. Nuzzo, P. Wiltzius, J. A. Lewis, *Adv. Mater.* **2009**, *21*, 2407.
[42] L. Brigo, A. Urciuolo, S. Giulitti, G. Della Giustina, M. Tromayer, R. Liska, N. Elvassore, G. Brusatin, *Acta Biomater.* **2017**, *55*, 373.
[43] E. Käpylä, T. Sedlačík, D. B. Aydogan, J. Viitanen, F. Rypáček, M. Kellomäki, *Mater. Sci. Eng., C* **2014**, *43*, 280.
[44] S. Nocentini, D. Martella, C. Parmeggiani, D. S. Wiersma, *Materials* **2016**, *9*, 525.
[45] I. Sakellari, E. Kabouraki, D. Gray, V. Purlys, C. Fotakis, A. Pikulin, N. Bityurin, M. Vamvakaki, M. Farsari, *ACS Nano* **2012**, *6*, 2302.
[46] J. Fischer, M. Wegener, *Laser Photonics Rev.* **2013**, *7*, 22.
[47] A. Pikulin, N. Bityurin, *Phys. Rev. B* **2007**, *75*, 195430.
[48] J. B. Mueller, J. Fischer, Y. J. Mange, T. Nann, M. Wegener, *Appl. Phys. Lett.* **2013**, *103*, 123107.
[49] K. Takada, K. Kaneko, Y. D. Li, S. Kawata, Q. D. Chen, H. B. Sun, *Appl. Phys. Lett.* **2008**, *92*, 041902.
[50] D. Martella, D. Antonioli, S. Nocentini, D. S. Wiersma, G. Galli, M. Laus, C. Parmeggiani, *RSC Adv.* **2017**, *7*, 19940.
[51] N. Uppal, P. S. Shiakolas, *J. Micro/Nanolithogr., MEMS, MOEMS* **2008**, *7*, 043002.
[52] C. Decker, K. Moussa, *Macromolecules* **1989**, *22*, 4455.
[53] S. C. Ligon, B. Husár, H. Wutzel, R. Holman, R. Liska, *Chem. Rev.* **2013**, *114*, 557.
[54] I. Staude, M. Thiel, S. Essig, C. Wolff, K. Busch, G. Von Freymann, M. Wegener, *Opt. Lett.* **2010**, *35*, 1094.
[55] R. A. M. Hikmet, D. J. Broer, *Polymer* **1991**, *32*, 1627.
[56] A. Žukauskas, I. Matulaitienė, D. Paipulas, G. Niaura, M. Malinauskas, R. Gadonas, *Laser Photonics Rev.* **2015**, *9*, 706.
[57] J. M. McCracken, V. P. Tondiglia, A. D. Auguste, N. P. Godman, B. R. Donovan, B. N. Bagnall, H. E. Fowler, C. M. Baxter, V. Matavulj, J. D. Berrigan, T. J. White, *Adv. Funct. Mater.* **2019**, *29*, 1903761.
[58] H. Zeng, D. Martella, P. Wasylczyk, G. Cerretti, J.-C. G. Lavocat, C.-H. Ho, C. Parmeggiani, D. S. Wiersma, *Adv. Mater.* **2014**, *26*, 2319.
[59] R. A. M. Hikmet, B. H. Zwerver, D. J. Broer, *Polymer* **1992**, *33*, 89.
[60] E. Anglaret, M. Brunet, B. Desbat, P. Keller, T. Buffeteau, *Macromolecules* **2005**, *38*, 4799.
[61] S. Hess, D. Frenkel, M. P. Allen, *Mol. Phys.* **1991**, *74*, 765.
[62] G. J. Kruger, *Phys. Rep.* **1982**, *82*, 229.
[63] S. V. Dvinskikh, I. Furó, H. Zimmermann, A. Maliniak, *Phys. Rev. E* **2002**, *65*, 061701.
[64] K. S. Chu, D. S. Moroi, *J. Phys., Colloq.* **1975**, *36*, C1.